

# Monitoring the growth of naturally regenerated vegetation after Typhoon Durian based on satellite image analysis

NGUYEN Thi To Ngan<sup>1,2</sup>, NGUYEN Thi Lan Thi<sup>1,2</sup>, NGO Thi Phuong Uyen<sup>1,2</sup>, NGUYEN Vinh Tung<sup>1,2</sup>, LIEU Kim Phuong<sup>3\*</sup>

<sup>1</sup> University of Science, Ho Chi Minh City, Vietnam

<sup>2</sup> Vietnam National University, Ho Chi Minh City, Vietnam

<sup>3</sup> Institute of Life Sciences, Vietnam Academy of Science and Technology, Ho Chi Minh City, Vietnam

\* Corresponding email: lkphuong@ils.vast.vn

**Abstract:** *Mangrove forests distributed in tropical and subtropical coastal areas are unique ecosystems and are very sensitive to changing environments. Mangrove forests are considered as a solid green wall to protect the coast, sea dykes, limit landslides and the harmful effects of typhoons. However, the area of mangrove forests in Vietnam is currently being seriously degraded, not only affecting human activities but also causing natural disasters such as typhoons and floods. On that edge, the impact of climate change makes the frequency and intensity of natural disasters from the sea increasingly high. The Typhoon Durian made landfall in the southern region of Vietnam, including Can Gio on April 12, 2006, caused many serious and dangerous damages, including many forest trees in Long Hoa commune that had been completely broken. The objective of this study is to use available satellite image data (SPOT, Landsat, Sentinel, and Google Earth) to generate forest maps from 2007 (after Typhoon Durian) to the present to assess the natural recovery rate in the areas affected by the typhoon in different conditions. The results can help foresters or environmentalists to build future forest status forums in the area.*

**Keywords:** *Remote sensing; Typhoon Durian; Natural regeneration; Climate change; Can Gio*

## 1. Introduction

Mangroves are common ecosystems in tropical and subtropical intertidal zones (B. F. Clough, 2013). They are distributed around the equator, from about 33 degrees north to 37 degrees south latitude (Walsh, 1974), and cover six different regions from east to west. These ecosystems provide a variety of ecological services and are important to humans. Although not a highly biodiverse ecosystem, mangroves are among the most biologically productive ecosystems in the world. Due to their longevity and large biomass, especially below-ground biomass (B. F. Clough, 2013), mangroves become an effective tool in reducing the amount of CO<sub>2</sub> released into the atmosphere - one of the main causes of climate change. The CO<sub>2</sub> absorption capacity of mangroves is believed to be higher than that of terrestrial ecosystems (B. Clough, 1998). In the context of climate change, which is increasing the frequency and intensity of marine disasters, the role of mangroves in coastal protection becomes increasingly important. The total area of mangroves globally is currently about 15 million hectares (Spalding, 2010), distributed across 118 tropical and subtropical countries and territories (Wilkie & Fortuna, 2003). However, the majority of mangroves (about 75%) are concentrated in 15 countries, and only 6.9% of the area is protected (Chandra et al., 2010). The area of mangrove forests worldwide is declining, especially in Asia, where the forest area decreased by 25% from 1980 to 2005. The most seriously affected countries are Indonesia, Pakistan, Vietnam, Malaysia, and India, with the main causes being the conversion of forest land into aquaculture ponds, salt production, rice cultivation, and environmental pollution (B. F. Clough, 2013). In Southeast Asia, from 2000 to 2012, the area of mangrove forests decreased by about 0.18% per year (Richards & Friess, 2015).

In addition to human activities, natural disasters such as storms and tsunamis also cause mangrove forest degradation, leaving serious and long-term ecological and environmental consequences, leading to socio-economic instability, especially in countries whose livelihoods are heavily dependent on nature, like Vietnam.

Many studies on the recovery of mangrove forests after storms have been conducted worldwide. For example, (Roth, 1992) described the impact and monitored the recovery of mangroves 17 months after Hurricane Joan in Nicaragua in 1988. Imbert et al. (Imbert, Labbe, & Rousteau, 1996) divided mangroves into three regions and studied the impact of Hurricane Hugo in 1989. Sherman et al. (Sherman, Fahey, & Martinez, 2001) studied the impact of Hurricane Georges in the Dominican Republic in 1998. Kauffman & Cole (Kauffman & Cole, 2010) studied the recovery of mangroves in Micronesia after Hurricane Sudal in

2004. Aung et al. (Aung, Mochida, & Than, 2013) studied the recovery after Hurricane Nargis in Myanmar in 2008.

Mangrove ecosystems are influenced by many environmental factors, which determine the richness, diversity, and productivity of each forest area. As forest productivity declines, biodiversity also declines, making the ecosystem vulnerable and less resilient to environmental impacts. Under the impact of storms, the amount of poor-quality organic matter (woody trunks, branches, leaves) increases suddenly, along with the loss of living plant cover, causing drastic changes in community structure and ecosystem function. Therefore, finding environmental treatment solutions to support the self-recovery process of mangrove forests is very necessary, although not simple. Excessive poor-quality organic matter can cause nutritional deficiencies, inhibiting plant growth. Large tree trunks and branches also hinder the growth of young trees. However, clearing these materials can change the temperature and humidity regime of the sediment, causing the forest to receive more solar radiation, which affects the recovery process. Therefore, examining and surveying the recovery of natural forests under different conditions—including (1) the forest area that was broken after the disaster but kept intact, called the “uncleared area”; (2) the forest area where the broken tree trunks were removed after the disaster, called the “cleared area”; and (3) the forest area where some large broken tree trunks were removed but part remained, called the “partially cleared area” (Diele et al., 2013)—will help environmental managers gain an overview. From there, they can make reasonable proposals and optimal solutions to handle the environment after the disaster while supporting sustainable forest management and improving the livelihoods of communities dependent on mangrove forests.

Humans have been using remote sensing technology since very early times. In 1860, James Wallace Black photographed parts of Boston from a hot air balloon. The development of science and technology has made remote sensing an important tool in observing and studying the Earth's surface. With the advancement of satellite and space technology, the types of remote sensing images are increasingly diverse, and the quality of data is also improving. In addition to traditional types of images such as low-resolution aerial photos or satellite images (SPOT-1, 2 or Landsat-1, 2, 3, 4) to medium resolution (Landsat-5, 7, 8, Sentinel-2 or SPOT-4, 5), today we also have high-quality remote sensing images such as SPOT-6/7, IKONOS, or WorldView. Medium-resolution satellite images play an important role in mapping forests over large geographical areas (Baumann et al., 2011; Feng, 2009; Liu et al., 2005; Shalaby & Tateishi, 2007; Yuan, Sawaya, Loeffelholz, & Bauer, 2005; Zhang, Tian, & Dang, 2011).. Globally, there have been many studies on extracting mangrove information from this type of medium-resolution remote sensing data (Nguyen, Truong, Ngo, Nguyen, & Lieu, 2023; Seto & Fragkias, 2007; Shalaby & Tateishi, 2007; Su-Fen Wang, 2004).

From the period of 1979-1980, Vietnamese state agencies began to approach remote sensing technology. In the next 10 years (1980-1990), research and experiments were conducted to determine the ability and methods of using remote sensing data to solve specific tasks. In Vietnam, the application of remote sensing and GIS to monitor mangrove changes has achieved many remarkable accomplishments (Nguyễn, Ngô, & Nguyễn, 2018; Tran, Nguyen, & Nguyen, 2017; Trần, Phùng, Phạm, & Lê, 2016).

In this study, to monitor and evaluate the rate of forest regeneration in the area affected by the 2006 Typhoon Durian in Can Gio, remote sensing and GIS data were integrated. The data were classified based on algorithms, and forest regeneration was observed under three different status conditions: (1) “uncleared area”, (2) “cleared area”, and (3) “partially cleared area”.

## 2. Study Area

Typhoon Durian made landfall in southern Vietnam on December 4, 2006, causing severe damage to life and property. The disaster killed at least 44 people, sank hundreds of fishing boats, and damaged many houses in the area. Long Hoa Commune, located in the south of Can Gio District, is famous in the tourism industry for the Sac Forest Conservation Area (Monkey Island) and the 30/4 Beach tourist area. It is 56.5 km from the center of Ho Chi Minh City by road. The study area is located in the southwest of Long Hoa Commune, bordering the Monkey Island tourist area to the north, the East Sea to the south, the Dong Tranh River to the west, and Sac Forest Road to the east.



**Fig. 1.** Study area

The objective of the study was to use remote sensing data and analytical techniques to extract information on forest status and collapsed areas before and after Typhoon Durian (2006) in order to create status maps. Based on these results, it is possible to compare and observe the regeneration of natural forests in the collapsed areas caused by the typhoon under two main cases: (1) the area cleared of all fallen tree trunks after the typhoon, called the "cleared area," and (2) the area left with fallen tree trunks on the surface, called the "uncleared area." In addition, there is an area that is partially cleared, called the "partially cleared area" (Figure 2).

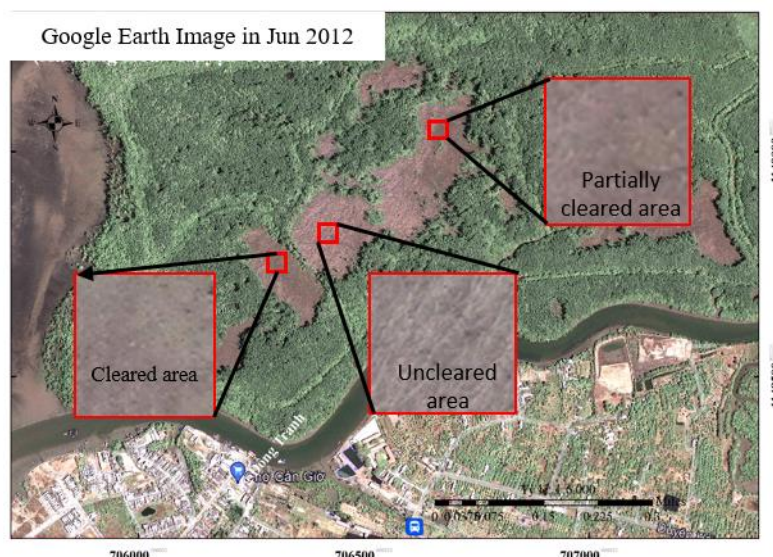


**Fig. 2.** Three different conditions of the natural forest regeneration after Typhoon Durian in Can Gio

### 3. Materials

Due to the heterogeneous operating times of satellites, some satellites have stopped operating permanently, such as Landsat-1 (which stopped operating in 1978), while others have errors, such as Landsat-7 ETM+ (which has had scan line errors since 2003) (Irons). To monitor the current status of forest loss caused by Typhoon Durian in 2006, the selected satellite images include Landsat-5, Landsat-8, Sentinel-2, and SPOT-2 and SPOT-5. Of these, Landsat data with processing level (Level 1A) is provided for free from the USGS (USA) Earth Explorer website. Sentinel-2 data is also provided for free from the Copernicus Data Space Ecosystem website, while SPOT images are provided by the National Remote Sensing Department under the Ministry of Natural Resources and Environment of Vietnam.

Table 1 presents information from the remote sensing datasets (Landsat-5, Landsat-8, Sentinel-2, SPOT-2, and SPOT-5) used to map the current status of typhoon-induced and post-typhoon broken during the period from 2007 to 2022. However, due to the medium resolution of Landsat (15-30 m) and Sentinel-2 (10-20 m) data, it is impossible to observe unrecovered areas when damages have an area smaller than one pixel. Therefore, Google Earth images (2009-2022) used to addition the above defect. Although this data is not continuous and complete, the image resolution quality is very high. Since this is not raw data, we do not use classification and model extraction techniques as with Landsat, Sentinel, or SPOT, but instead perform visual interpretation on Google Earth. The interpreted information is then converted into digital data so that it can be overlaid with other datasets.

**Tab. 1.** Satellite image data used in this research.

Date	Landsat-5	Landsat-8	SPOT-2	SPOT-5	Sentinel-2	Google Earth
2004/01/18				S5_277329_20040118		
2005/02/22	LT05_L1TP_124053_20050222					
2007/01/27	LT05_L1TP_124053_20070127					
2007/12/05			S2_277329_20071205			
2008/01/21			S2_277329_20080121			
2008/12/22	LT05_L1TP_124053_20081222					
2009/04/19				S5_276329_20090419		
2009/12/18	LT05_L1TP_124053_20091218					
2009/12						x
2010/02/04	LT05_L1TP_124053_20100204					
2010/02						x
2010/03/14				S5_277329_20100314		
2011/01/06	LT05_L1TP_124053_20110106					
2011/11/23				S5_277329_20111123		
2012/02/14				S5_276329_20120214		
2013/10/26		LC08_L1TP_124053_20131026				
2014/03						x
2014/11/14		LC08_L1TP_124053_20141114				
2014/09						x
2015/12/03		LC08_L1TP_124053_20151203				
2016/01/14					S2A_MSIL2A_20160114T_032322_N0201_R075	
2016/03						x
2017/01/08					S2A_MSIL2A_20170108_T032301_N0500_R075	
2017/01						x
2018/01						x
2018/02/12					S2A_MSIL2A_20180212_T030831_N0500_R075	
2019/01						x
2019/02/27					S2A_MSIL2A_20190227_T030651_N0500_R075	
2019/9						x

2020/01/13					S2A_MSIL2A_20200113T 031101_N0500_R075	
2021/01/07					S2A_MSIL2A_20210107 T031121_N0500_R075	
2022/01/22					S2A_MSIL2A_20220122 T031021_N9999_R075	
2022/03						x

#### 4. Methodology

Figures 3a&b describe the steps involved in the creation of thematic maps (forest maps, storm-damaged area maps). Since the image sets are collected from many different sources, before being used for analysis and building a data extraction model, the satellite images must be rectified to the same WGS84 reference system using ground control points (GCPs).

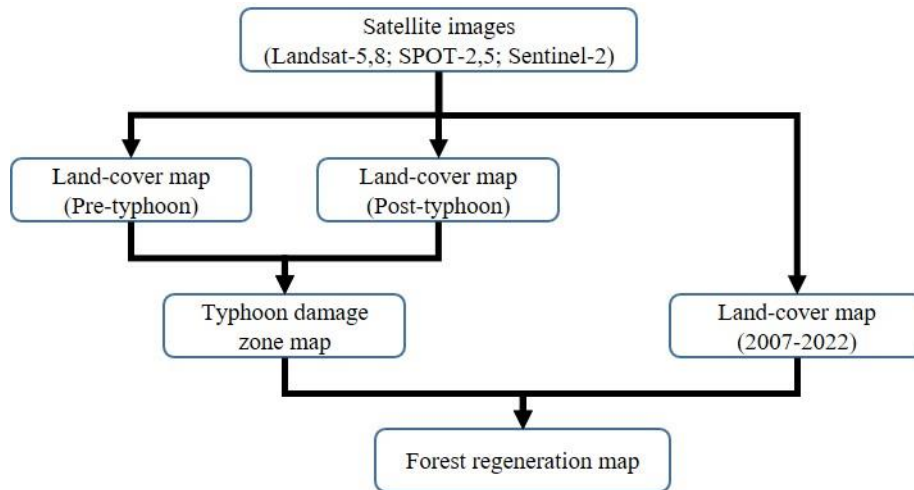


**Fig. 3a.** Flowchart of the research.

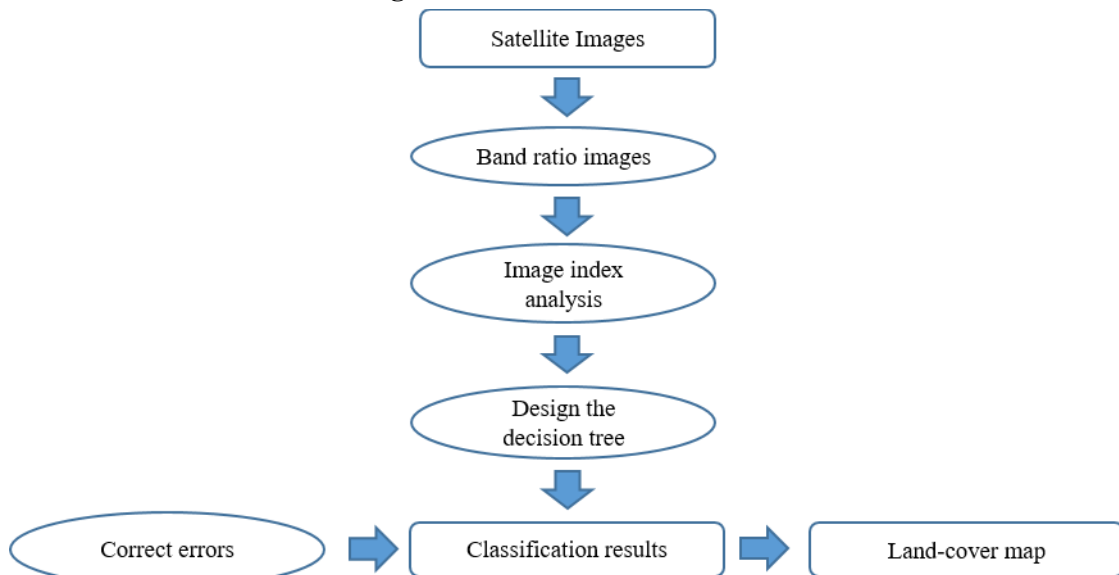


**Fig. 3b.** Steps of analyzing images to produce the land-cover map.

As is known, each wavelength has its own strengths and limitations in providing information about land surface units (vegetation, water, and soil). Therefore, to extract information about forests (vegetation) and typhoon-induced damaged (bare land) from remote sensing datasets in the study area, indices such as NDVI (highlighting vegetation area - Formula 1), NDWI (highlighting water area - Formula 2), NDSI (highlighting land area - Formula 3), along with UI and ReUI (highlighting built-up area - Formulas 4 and 5) were created. Then, based on the correlation between the interpreted objects (forest, landslide area) and the image indices, the classification thresholds for each specific index were determined. Finally, depended on these classification thresholds, a "decision tree" model was designed to extract the land surface information. The maps of forest coverage and damaged zone areas were generated by year to monitor the changes in damaged zone caused by the typhoon, fallen tree areas after the event (Typhoon Durian), and natural forest regeneration under different conditions.

$$NDVI = \frac{NIR-RED}{NIR+RED} \quad \text{(Formula 1)}$$

$$NDWI = \frac{GREEN-NIR}{GREEN+NIR} \quad \text{(Formula 2)}$$

$$NDSI = \frac{GREEN-SWIR}{GREEN+SWIR} \quad \text{(Formula 3)}$$

$$UI = \frac{GREEN}{SWIR2} \tag{Formula 4}$$

$$ReUI = \frac{SWIR2}{GREEN} \tag{Formula 5}$$

### 5. Results and Discussion

The results of monitoring the current status of forest destruction caused by Typhoon Durian in 2006 are divided into three stages:

#### 5.1 Damaged zones Caused by Typhoon Durian

The damaged areas caused by Typhoon Durian include the largest damaged area, which is also the main research area for natural regeneration according to the three conditions of the study that mentioned above, with an area of 5.67 ha, distributed in the southwest. In addition, there are a number of smaller damaged areas (ranging from 900 m<sup>2</sup> to 2,700 m<sup>2</sup>) located in the northwest of the survey area (Figure 2).

#### 5.2 Damaged Areas Expanded After the Typhoon Event

When comparing the current map of damaged areas from Typhoon Durian (December 2006) to April 2009, it shows that there was an increase in the area of damaged regions after the event (Table 2). During the period from 2006 to 2007, some relatively large areas of fracture expansion developed in the north. The largest area of expansion (15,140.01 m<sup>2</sup>) appeared in the southeast of the main study area (the largest fracture area). Smaller areas of expansion occurred on the edge of the main study area.

**Tab. 2.** Statistical table of damaged area in the period 2004-2019

	Year	Damaged zone area by typhoon (m <sup>2</sup> )
Pre-typhoon Durian	2004-2005	70.361,54
	26/12/2006	130.229,12
Damages by typhoon	2007	152.149,30
	2008	179.505,99
Increased collapse area post typhoon	04/2009	139.604,09
	12/2009	139.604,09
Natural forest regeneration post typhoon	2010	133.979,30
	2011	125.754,35
	2012	52.655,01
	2014	32.334,63
	2015	30.116,95
	2016	11.957,32
	2017	4.369,77
	2018	672,10
	2019	672,10
	2020	0

After this period (from December 26, 2006, to April 4, 2009), the expansion of the post-storm fracture area stopped, and at the same time, the regeneration process began. This is clearly shown by the narrowing of the fracture area (or the increase in forest area) in the study area from February 2010 to September 2020.

#### 5.3 Narrowing Damaged Area and the Development of Naturally Regenerating Forest

After April 2009, the damaged areas in the study area began to have regenerating forest. Based on the observation of the gradual narrowing of the damaged area, we can see that forest regeneration starts

from the edge of the damaged zone areas and gradually moves toward the center (Figure 4). The “cleared area” was covered with regenerated forest the earliest (in 2016), followed by the “partially cleared area” (in 2009). By September 2019, there were still about 3,813.58 m<sup>2</sup> of the “uncleared area” without regrowth. Figure 4 shows the progress of forest regeneration over the years (from April 2009 to September 2019). In the main study area, we found that the regenerated forest in the “uncleared area” tended to develop in the northeast-southwest direction.

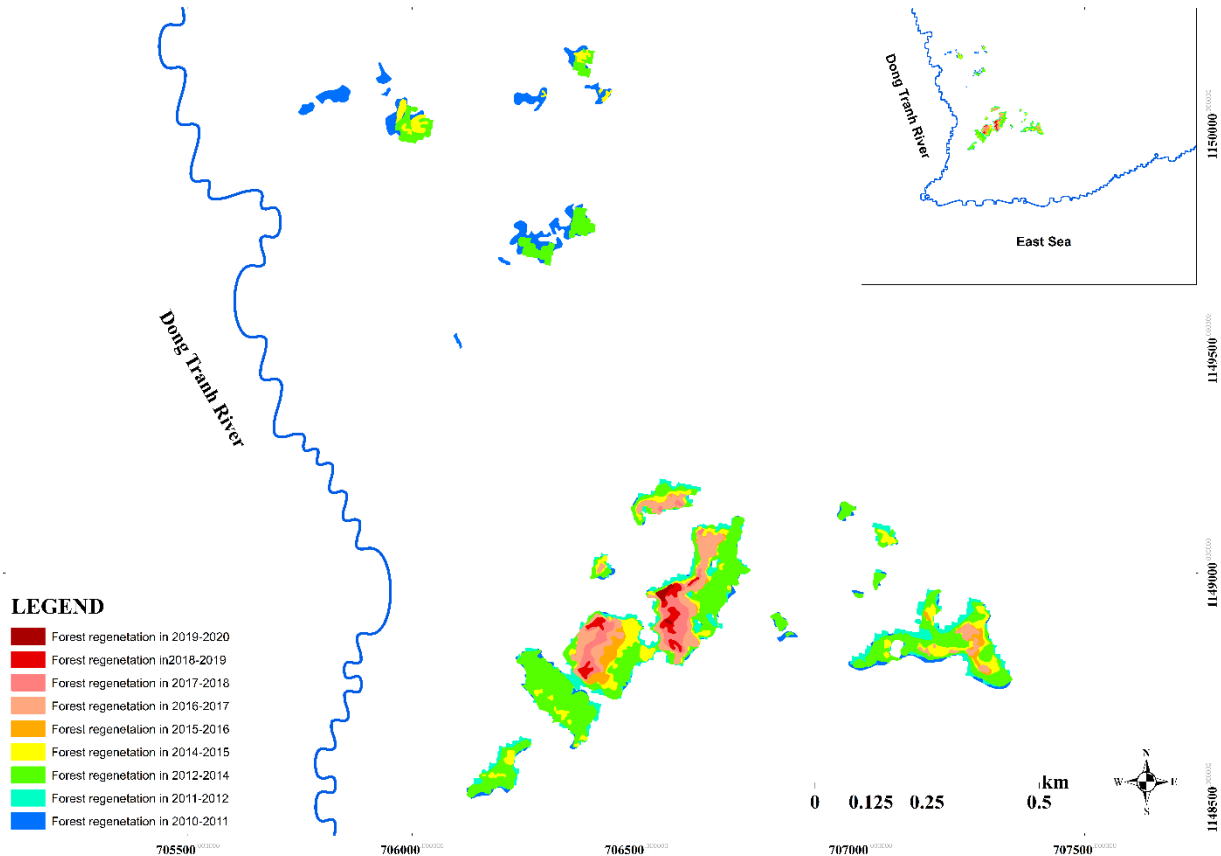


**Fig. 4.** The natural forest regeneration post typhoon map (from 2009 to 2020)

Observations from Google Earth images show that forest recovery in the two types of damaged areas is different. Although the “cleared area” recovered faster than the other two areas, the canopy density appeared to develop more slowly, as indicated by the lighter green color of the forest in this area compared to the other two areas (Figure 5). The difference of the canopy density also showed that natural forest regeneration in the “uncleared area” occurs more slowly, but the diversity in the “uncleared area” is better developed which is reflected in species diversity (both *Rhizophora* and *Avicennia* grow here), while in the “cleared area” only *Avicennia* grow.

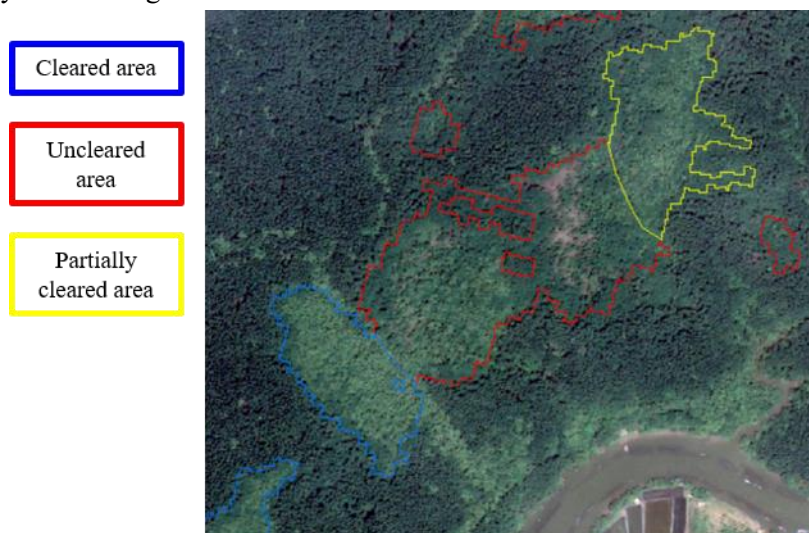


**Fig. 5.** Difference in canopy density of regenerating forest between “cleared area” (blue – low density) and “uncleared area” (red – high density).

## 6. Conclusion

The purpose of the project is to use remote sensing datasets to establish a map of forest status and areas of damage caused by Typhoon Durian in 2006, using the decision tree method. In this project, image classification models employing the decision tree method have demonstrated their effectiveness in the interpretation process when comparing the raw interpretation results with the complete forest status map.

Although the project encountered some shortcomings due to the heterogeneous resolution of the satellite image datasets used for analysis and interpretation (including resolutions ranging from low to medium, such as Landsat-5 and Landsat-8, to medium, such as SPOT-2 and Sentinel, and relatively high, such as SPOT-5), we combined the use of Google Earth (GE) image data, which has very high resolution (from a few meters to less than 1 m), to support the assessment of the status for the periods from 2009 to 2020. In general, the analysis results still meet the initial requirements.

Based on the observation of the regeneration process, we found that regeneration here develops in an east-west direction and has a northeast-southwest direction. Although the area of the two types of damaged areas (“cleared area” and “uncleared area”) differs significantly, making it subjective to evaluate which type progresses faster than the other, in terms of biodiversity, the research team found that maintaining the current state of the damaged area (“Uncleared area”) is still more positive than clearing the damaged area (“Cleared area”). In addition, Natural forest regeneration in the "uncleared area" occurs more slowly, but the diversity in the "uncleared area" is better developed which is reflected in species diversity (both *Rhizophora* and *Avicennia* grow here), while in the "cleared area" only *Avicennia* grow. However, to conclude more accurately about this regeneration rate, we aim to review and analyze the correlation between factors such as flow, terrain elevation, and tides in relation to this natural regeneration process.

**Conflicts of Interest: The authors declare no conflict of interest.**

## Acknowledgements

This research is funded by Vietnam National University, Ho Chi Minh City (VNU-HCM) under grant number B2025-18-10.

## Literature - References

1. Aung, T., Mochida, Y., & Than, M. (2013). Prediction of recovery pathways of cyclone-disturbed mangroves in the mega delta of Myanmar. *Forest Ecology and Management*, 293, 103–113. doi: 10.1016/j.foreco.2012.12.034
2. Baumann, M., Kuemmerle, T., Elbakidze, M., Ozdogan, M., Radeloff, V. C., Keuler, N. S., . . . Hostert, P. (2011). Patterns and drivers of post-socialist farmland abandonment in Western Ukraine. *Land Use Policy*, 28(3), 552-562.
3. Chandra, G., Ochieng, E., Tieszen, L., Zhu, Z., Singh, A., Loveland, T., . . . Duke, N. (2010). Status and distribution of mangrove forest of the world using earth observation satellite data. *Global Ecology and Biogeography*, 20, 154-159. doi: 10.1111/j.1466-8238.2010.00584.x
4. Clough, B. (1998). Mangrove forest productivity and biomass accumulation in Hinchinbrook Channel, Australia. *Mangroves and Salt Marshes*, 2(4), 191-198. doi: 10.1023/A:1009979610871
5. Clough, B. F. (2013). CONTINUING THE JOURNEY AMONGST MANGROVES.
6. Diele, K., Ngoc, D. M., Geist, S., Meyer, F., Huong, P., Saint-Paul, U., . . . Berger, U. (2013). Impact of typhoon disturbance on the diversity of key ecosystem engineers in a monoculture mangrove forest plantation, Can Gio Biosphere Reserve, Vietnam. *Global and Planetary Change*, 110, 236-248. doi: 10.1016/j.gloplacha.2012.09.003
7. Feng, L. (2009). Applying remote sensing and GIS on monitoring and measuring urban sprawl. A case study of China. *Revista Internacional Sostenibilidad, Tecnología y Humanismo*(4), 47-56.
8. Imbert, D., Labbe, P., & Rousteau, A. (1996). Hurricane damage and forest structure in Guadeloupe, French West Indies. *Journal of Tropical Ecology*, 12(5), 663-680.
9. Irons, N. O. J. R. The Multispectral Scanner System Retrieved 29 June, 2016, from <http://landsat.gsfc.nasa.gov/?p=3227>
10. Kauffman, J. B., & Cole, T. G. (2010). Micronesian Mangrove Forest Structure and Tree Responses to a Severe Typhoon. *Wetlands*, 30(6), 1077-1084. doi: 10.1007/s13157-010-0114-y

10. Liu, J., Liu, M., Tian, H., Zhuang, D., Zhang, Z., Zhang, W., . . . Deng, X. (2005). Spatial and temporal patterns of China's cropland during 1990–2000: an analysis based on Landsat TM data. *Remote sensing of Environment*, 98(4), 442-456.
11. Nguyễn, T. T. N., Ngô, T. P. U., & Nguyễn, T. M. T. (2018). Modelling to extract land cover information from Landsat satellite images - A case study in Ba Tri district, Ben Tre province. Vietnam.
12. Nguyen, T. T. N., Truong, T. H. H., Ngo, T. P. U., Nguyen, T. L. T., & Lieu, K. P. (2023). Extracting Land-Cover Information from Landsat Satellite Images by the Decision-Tree Model to Generate a Land-Use Map in Ba Tri District, Ben Tre Province. *Research & Development*, 4(3), 102-110. doi: 10.11648/j.rd.20230403.15
13. Richards, D., & Friess, D. (2015). Rates and drivers of mangrove deforestation in Southeast Asia, 2000–2012. *Proceedings of the National Academy of Sciences*, 113, 201510272. doi: 10.1073/pnas.1510272113
14. Roth, L. C. (1992). Hurricanes and Mangrove Regeneration: Effects of Hurricane Joan, October 1988, on the Vegetation of Isla del Venado, Bluefields, Nicaragua. *Biotropica*, 24, 375-384.
15. Seto, K. C., & Fragkias, M. (2007). Mangrove conversion and aquaculture development in Vietnam: A remote sensing-based approach for evaluating the Ramsar Convention on Wetlands. *Global Environmental Change*, 17(3), 486-500.
16. Shalaby, A., & Tateishi, R. (2007). Remote sensing and GIS for mapping and monitoring land cover and land-use changes in the Northwestern coastal zone of Egypt. *Applied Geography*, 27(1), 28-41.
17. Sherman, R., Fahey, T., & Martinez, P. (2001). Hurricane Impacts on a Mangrove Forest in the Dominican Republic: Damage Patterns and Early Recovery<sup>1</sup>. *Biotropica*, 33, 393-408. doi: 10.1111/j.1744-7429.2001.tb00194.x
18. Spalding, M. (2010). *World atlas of mangroves*: Routledge.
19. Su-Fen Wang, C.-C. C., Yeong - Kuan Chen. (2004). Forest cover type classification using Spot 4 and Spot 5 Images.
20. Tran, B., Nguyen, L., & Nguyen, K. (2017). APPLICATION OF GIS AND REMOTE SENSING IN ANALYZING THE CURRENT STATUS AND ASSESSING THE CHANGE OF FOREST RESOURCES IN VINH CUU DISTRICT, DONG NAI PROVINCE. 06.
21. Trần, T. H., Phùng, M. T., Phạm, T. Q., & Lê, T. G. (2016). Application of GIS and Remote Sensing in monitoring forest area changes in Cao Phong district, Hoa Binh province, period 2005-2015 *Journal of Science and Technology*, 4, 59-69.
22. Walsh, G. E. (1974). MANGROVES: A REVIEW<sup>1</sup>.
23. Wilkie, M. L., & Fortuna, S. (2003). Status and trends in mangrove area extent worldwide.
24. Yuan, F., Sawaya, K. E., Loeffelholz, B. C., & Bauer, M. E. (2005). Land cover classification and change analysis of the Twin Cities (Minnesota) Metropolitan Area by multitemporal Landsat remote sensing. *Remote sensing of Environment*, 98(2), 317-328.
25. Zhang, Z., Tian, S., & Dang, W. (2011). Study of Wetland Information Enhancement Approach Based on Landsat Etm Data. *ISPRS-International Archives of the Photogrammetry, Remote Sensing and Spatial Information Sciences*, 3825, 150-152.